

From Oil-Swollen Wormlike Micelles to Microemulsion Droplets: A Static Light Scattering Study of the L_1 Phase of the System Water + $C_{12}E_5$ + Decane

U. Menge, P. Lang,* and G. H. Findenegg

Iwan-N.-Stranski-Institut für Physikalische und Theoretische Chemie, Technische Universität Berlin, Strasse des 17. Juni 112, D-10623 Berlin, Germany

Received: January 8, 1999

The microstructure of the ternary system pentaethyleneglycol monododecyl ether ($C_{12}E_5$), decane and water was investigated by static light scattering in the water-rich region of the phase diagram at constant temperature (22 °C). Micellar size and shape were determined along several pseudobinary sections of constant oil-to-surfactant ratio. The main focus was on dilute solutions (c_m ranging from 0.0004 g cm⁻³ up to 0.3 g cm⁻³, where c_m denotes the mass concentration of oil plus surfactant in the aqueous phase) and small oil content (α up to 0.35, where α denotes the mass fraction of oil in the oil + surfactant mixture). Our data analysis supports the presumed existence of wormlike micelles at low α . The concentration dependence of the apparent molar mass M_{app} of the micelles can be represented over a wide concentration range (up to the semidilute regime) by a model that combines a power law $M_w \propto c_m^a$ with the structure factor $S(q = 0)$ for flexible polymer chains in good solvents. For $\alpha \leq 0.10$ the fitted value of the growth exponent a agrees with the mean-field prediction ($a \approx 0.5$). With increasing oil content at given overall solute concentration c_m the molar mass M_w of the micelles increases up to a maximum near $\alpha = 0.07$ but decreases rapidly as the oil content is further increased. This decrease of M_w is due to a transition from elongated (wormlike) micelles to microemulsion droplets. At high oil content ($\alpha = 0.35$) the data can be represented by a model of spherical droplets interacting like hard spheres.

1. Introduction

It is well-established that micellar systems can exhibit unidimensional micellar growth in the isotropic micellar phase (L_1 phase). Microscopically, the micellar growth is driven by the free energy difference between surfactant molecules in the cylindrical body of the micelle and molecules located at the energetically unfavorable spherical end caps of the micelle. At concentrations above the critical micelle concentration, mean field theory predicts a length distribution of the micelles that is essentially exponential. Furthermore, the mean length \bar{L} of uncharged micelles will show a concentration dependence that may be written as $\bar{L} \propto c^a$, where $a \approx 0.5$.^{1,2} Due to thermal motions, a long tubular aggregate will exhibit some degree of flexibility resulting in a wormlike micelle that is rigid only on a length scale $l < l_p$ where l_p is the persistence length. The surfactant concentration being sufficiently high, the wormlike micelles entangle and form a transient network, where many static and dynamic properties follow the universal scaling laws of semidilute polymer solutions.^{1,3} At higher dilution, however, nonuniversal properties of the system will combine with general behavior like the expected mean-field concentration dependence of the micellar contour length \bar{L} or the weight-average micellar mass M_w being proportional to \bar{L} . Recent experimental investigation of the growth in various micellar systems led to contradicting results regarding the growth exponent in the concentration dependence of the micellar mass, $M_w \propto c^a$. For highly dilute aqueous solutions of $C_{12}E_6$, the mean field exponent $a = 0.5$ was verified at several temperatures,⁴ and the same result was found for ionic surfactants at high ionic

strength of the solvent.^{5,6} Conversely, a higher growth exponent, $a \approx 1.1$ – 1.2 , was observed in dilute aqueous solutions of $C_{16}E_6$,⁷ of $C_{16}TAB$ – $C_{12}E_6$ mixed micelles,⁸ and in lecithin water-in-oil microemulsions.⁹

The size and shape of $C_{12}E_5$ micelles in aqueous solutions has been studied by many investigators using various techniques.^{10–14} In particular, it was demonstrated that even at low concentrations $C_{12}E_5$ aggregates into elongated micelles that grow with increasing concentration.¹⁰ Above the overlap concentration c^* the system follows the scaling laws for polymers with good solvents in the semidilute regime.¹⁴ This scaling behavior was observed even at temperatures very close to the critical temperature T_c , which is at about 32.0 °C for $C_{12}E_5$ –H₂O.¹⁶ It was anticipated that results from light scattering experiments conducted more than this away from the phase separation curve would reflect micellar properties rather than critical fluctuations. Accordingly, for our investigations of the ternary system $C_{12}E_5$, decane, and water at room temperature we took the binary system $C_{12}E_5$ –water as a reference system for wormlike micellar structures.

In this study we have investigated the microstructure of the isotropic micellar L_1 phase in the ternary system $C_{12}E_5$, decane, and water in the water-rich corner of the phase prism at $T = 22$ °C. The addition of a hydrocarbon oil like decane to the binary $C_{12}E_5$ –water system has a pronounced effect on the micellar shape in the L_1 phase. When the oil-to-surfactant ratio is very low, we can assume that the oil is solubilized inside the hydrocarbon core of the micelles without changing the preferential organization of the surfactant into wormlike micelles. With increasing oil-to-surfactant ratio, however, an oil-in-water microemulsion will eventually form. Specifically, the composition–temperature phase diagram for a mixture of decane +

* Corresponding author. Phone: (+49)-30-31422750. Fax: (+49)-30-31426602. E-mail: lang0630@mailszrz.zrz.tu-berlin.de.

surfactant with a constant ratio of 48.1/51.9 by weight against water was investigated in detail.¹⁷ In such a pseudobinary phase diagram the L₁ phase is bounded by a two-phase region below 25 °C, where the L₁ phase coexists with an excess oil phase. It was shown that at temperatures slightly above this emulsification failure spherical oil-swollen micelles (microemulsion droplets) are present that do not grow with the concentration of the solute oil–surfactant mixture.¹⁸ Thus, as one moves from the binary system C₁₂E₅–water into the phase prism toward the lower two-phase region, the micellar shape is transformed from wormlike into globular structures at constant temperature. This is in agreement with calculations based on the flexible surface model for water–surfactant–oil mixtures where the range of stability of spherical and cylindrical micelles was investigated as a function of the surfactant film properties and the composition of the system. It was found that with increasing oil-to-surfactant ratio the micellar structure changes from elongated cylinders to microemulsion droplets, until at high oil content the emulsification failure with an oil excess phase is observed.¹⁹ The aim of this work was to monitor this change in micellar structure with increasing oil content of the solute at constant temperature. In particular, we wanted to determine the range of stability of wormlike micelles with respect to the solute oil content and verify the predicted mean-field power law dependence of the micellar growth on the concentration of the dissolved oil–surfactant mixture at high dilution. Thus, the focus of this study is on dilute aqueous systems of C₁₂E₅ and decane at low oil content.

2. Experimental Section

Materials. High-purity pentaethyleneglycol monododecyl ether (C₁₂E₅) was purchased from Nikko and used as received. Decane (>98%) was obtained from Fluka. High-purity water from a Milli-Q-system (Millipore Systems) was used as a solvent.

Preparation of the Solutions. Several stock solutions were prepared by dissolving different mixtures of C₁₂E₅ and decane in water. The mass fraction of decane in the decane + C₁₂E₅ mixtures is denoted as α from now on. The ternary systems investigated had a solute oil content $\alpha = 0.02, 0.05, 0.07, 0.10, 0.15, 0.25$, and 0.35 . We also investigated the binary system C₁₂E₅–water ($\alpha = 0$) for comparison. For each system, the micellar concentration of the solute, denoted c_m , was varied in a wide concentration range by diluting the stock solutions with water. Figure 1 shows the parameters α and c_m in a cut through the phase prism at constant temperature. In order to remove dust from the solutions, they were filtered through millipore filters (0.2 μ m) directly into dust free quartz cuvettes with an inner diameter of 0.8 cm. To avoid a change in concentration due to filtration, the first milliliters of the filtrate were discarded.

Cloud Point Curve Determination. The addition of small amounts of oil to aqueous solutions of C_nE_m leads to a lowering of the cloud curve.²⁰ Since the light scattering measurements were performed at constant temperature, the demixing curves at a given α had to be determined. A portion of each solution was transferred into screw-topped test tubes, and the cloud curve was determined by visual inspection in a look-through water bath with a temperature control better than 0.01 K. The cloud curves for $\alpha \leq 0.10$ showed a distinct minimum at a solute concentration of about 0.015 g cm⁻³, whereas for $\alpha \geq 0.15$ a minimum of the cloud curve could not be unambiguously identified. With increasing solute oil content, the cloud curve was shifted to lower temperatures but increased again at higher

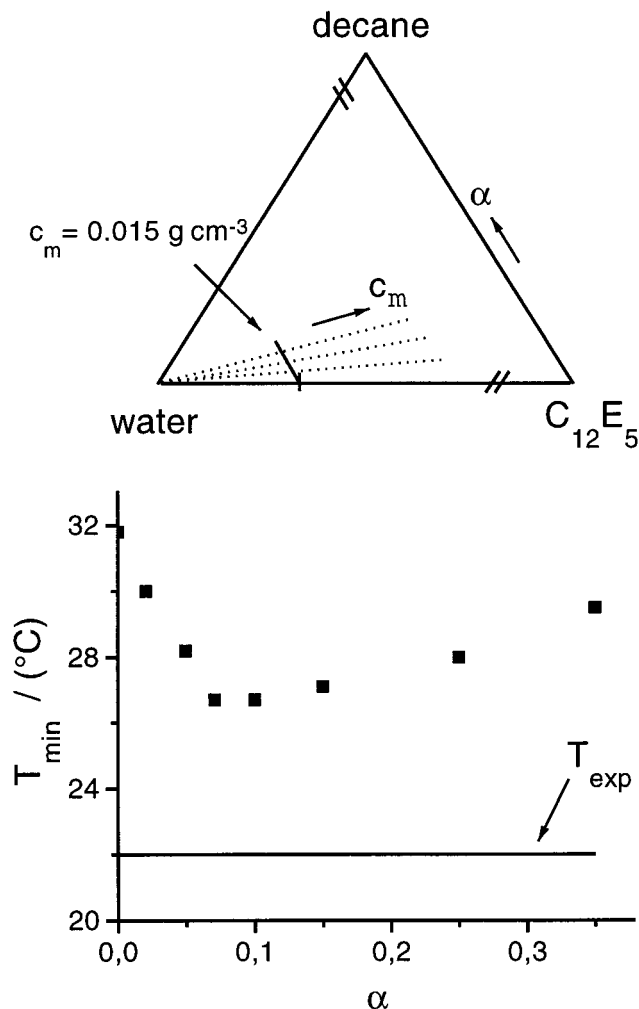


Figure 1. Schematic phase diagram showing quasi-binary paths in the ternary system water + C₁₂E₅ + decane (dotted lines). α denotes the mass fraction of decane in the decane + C₁₂E₅ solute mixture, and c_m is the mass concentration of the mixed solute along a pseudobinary path. The lower diagram shows the phase separation temperature T_{\min} at $c_m = 0.015$ g cm⁻³ as a function of α . All light scattering experiments were performed at 22 °C.

TABLE 1: Minimum of the Cloud Point Curves T_{\min} and Refractive Index Increment dn/dc at $T = 22$ °C for Different Solute Oil Content α

α	0	0.02	0.05	0.07	0.10	0.15	0.25	0.35
T_{\min} , °C	31.8	30.0	28.2	26.7	26.7	27.1	28.0	29.5
dn/dc , cm ³ /g	0.131	0.129	0.127	0.125	0.126	0.124	0.120	0.120

α (Figure 1). The minimum temperature of the phase boundary curve for several values of α at a solute concentration $c_m = 0.015$ g cm⁻³ is given in Table 1.

Light Scattering Measurements. The scattering experiments were performed with a commercial setup (ALV, Langen) that allows simultaneous measurements of static and dynamic light scattering. The light source was an argon laser (Coherent) operating at the blue line (488 nm) at a power output of 100 mW. For samples with higher scattering powers an attenuator was employed. A beam splitter and a four-segment photodiode were used to adjust the primary laser beam position and to monitor the beam intensity. The sample temperature was kept constant at 22 °C within ± 0.02 K using a toluene thermostating bath that also index-matched the quartz cuvettes containing the samples. Absolute calibration of the instrument was made with toluene (Fluka, >99.5%).

In the static LS experiments, the scattering angle was varied from 20° to 150° in 5° steps covering a range in scattering vectors q from 5.96×10^4 to $3.34 \times 10^5 \text{ cm}^{-1}$ with $q = (4\pi n/\lambda_0) \sin(\theta/2)$ depending slightly on the sample concentration. Reduced integrated excess intensities $R(q)$ were derived from the relative scattered intensities $r(q) = i(q)/I_0$ by taking into account the solvent background and the scattering power of toluene, viz.

$$R(q) = \frac{r(q) - r_0(q)}{r_{\text{Tol}}(q)} \left(\frac{n}{n_{\text{Tol}}} \right)^2 R_{\text{vv}}$$

where $r_0(q)$ and $r_{\text{Tol}}(q)$ refer to the pure solvent (water) and toluene, respectively, R_{vv} is the absolute scattering power of toluene, and $(n/n_{\text{Tol}})^2$ is a correction factor for the scattering volume appropriate for our setup.²¹ In the calculations of the quantity $Kc_m/R(q)$, the mass concentration of the micellar solution was corrected for the critical micelle concentration (c_{cmc}) using $c_m = c - c_{\text{cmc}}$. We neglected the dependence of the c_{cmc} on the oil content α and took the value of the pure surfactant ($c_{\text{cmc}} = 0.029 \text{ mg cm}^{-3}$)¹⁶ for all solutions. The optical contrast factor K was calculated on the basis of measured values of the refractive index increment dn/dc at the experimental wavelength. These values were measured using a Brice–Phoenix differential refractometer that had been calibrated with aqueous solutions of potassium chloride and sodium chloride. Experimental values of dn/dc as a function of α are summarized in Table 1.

The q dependence of the reduced scattering intensity $Kc_m/R(q)$ was found to be strictly linear in q^2 for almost all samples. Deviations occurred at high solute concentrations ($c_m \geq 0.1 \text{ g cm}^{-3}$ for $\alpha = 0.10$ and $\alpha = 0.15$) at low q . Here only the data at higher scattering vector were linear in q^2 . Extrapolation to zero scattering vector yielded the apparent molar mass M_{app}

$$M_{\text{app}}(c_m) = \left(\lim_{q^2 \rightarrow 0} \frac{Kc_m}{R(q)} \right)^{-1} = M_w(c_m) S(c_m, q=0) \quad (1)$$

which is the product of the weight-average molar mass of the micelles, M_w , and the concentration-dependent structure factor at zero scattering vector, $S(c_m, q=0)$. Since for micellar solutions M_w can change with concentration, the full concentration dependence of M_{app} at constant α has to be analyzed.

3. Results and Discussion

Figure 2 shows the dependence of the apparent molar mass M_{app} on the solute concentration c_m for three quasi-binary sections of low oil content α . The binary system C_{12}E_5 –water without oil ($\alpha = 0$) is also shown for comparison. For each data set the apparent molar mass is large even at the lowest concentration of the mixed solute. As the concentration c_m is increased, a pronounced maximum of M_{app} occurs at a concentration between 4 and 8 mg cm^{-3} , and a rapid decrease of M_{app} at higher concentrations. Considering the fact that the apparent aggregation number of the micelles of C_{12}E_5 at the lowest concentration (≈ 1200) is already much higher than typical values for spherical micelles, the data reflect micellar growth of elongated micelles with increasing concentration, which is eventually overruled by the concentration dependence of the structure factor $S(c_m, q=0)$, leading to a decrease in M_{app} at higher concentrations. Given the small oil content of the solute in the systems presented in Figure 2, we anticipate that the micellar structure is wormlike as in the binary system. We note that in this regime of low oil content M_{app} increases with

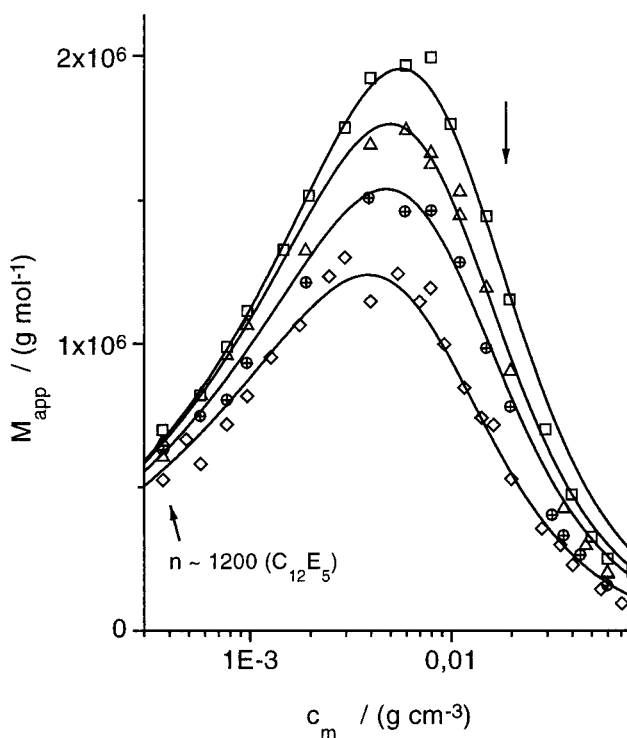


Figure 2. M_{app} vs c_m for $\alpha \leq 0.07$ at 22 °C. Experimental data: (\diamond) $\alpha = 0$; (\oplus) $\alpha = 0.02$; (\triangle) $\alpha = 0.05$; (\square) $\alpha = 0.07$. The solid lines represent fits based on the model of flexible wormlike micelles in dilute solutions; the arrow indicates the crossover concentration into the semidilute regime. The apparent aggregation number n for C_{12}E_5 at the lowest experimental concentration in pure water is also indicated.

increasing α over the whole concentration range investigated, and the maximum of M_{app} is shifted to higher concentrations as α is increased.

When the oil content α in the solute mixture is further increased, the concentration dependence of M_{app} is gradually changing (Figures 3 and 4). In the low solute concentration regime, the M_{app} vs c_m curves are systematically shifted to lower M_{app} when the solute oil content is increased from $\alpha = 0.07$ to $\alpha = 0.15$. This indicates a reduced tendency to micellar growth when more oil is incorporated in the micelles. At $\alpha = 0.10$ and $\alpha = 0.15$, the concentration dependence of M_{app} is qualitatively still similar to that at $\alpha \leq 0.07$. At $\alpha = 0.25$, however, only a weak maximum of M_{app} appears; finally, at $\alpha = 0.35$ (corresponding approximately to a relative molar composition decane:surfactant = 3:2), the apparent molar mass decreases monotonically with the solute concentration. Such a behavior is expected for spherical particles of constant size interacting with each other as hard spheres.

These observations suggest that the isotropic micellar L_1 phase contains wormlike micelles up to 10–15% oil content of the oil + surfactant mixed solute. The mass of the wormlike micelles is largest near $\alpha = 0.07$ and drops considerably as the oil content in the mixed solute is increased further. At $\alpha = 0.35$, the micellar structure has apparently transformed into a droplet microemulsion. Below the results for the low-oil-content regime (oil-swollen wormlike micelles) and those for the high-oil-content regime (droplet microemulsions) will be treated separately in terms of quantitative models.

Low Solute Oil Content. The concentration dependence of the apparent molar mass at low solute oil content is now analyzed in the framework of wormlike micelles, drawing on the analogy to the well-characterized binary system C_{12}E_5 in water. We use the analogy between wormlike micelles and

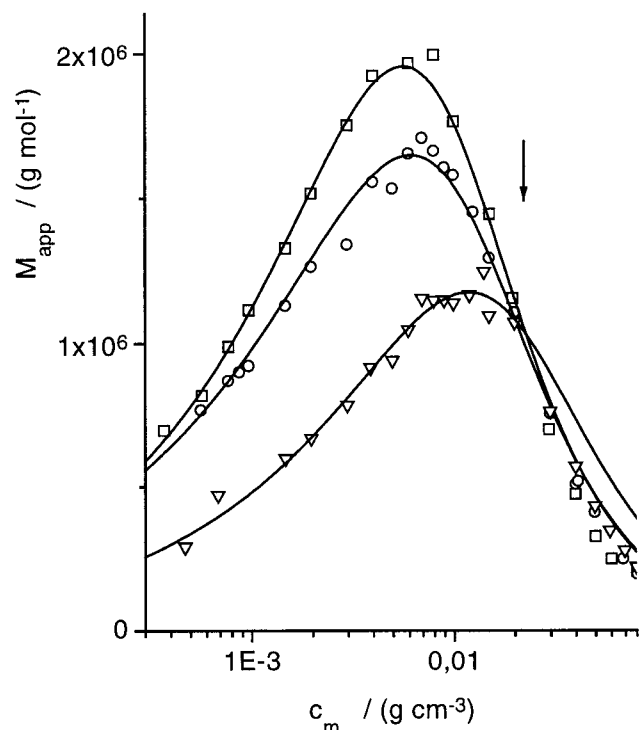


Figure 3. M_{app} vs c_m for $0.07 \leq \alpha \leq 0.15$ at 22 °C. Experimental data: (\square) $\alpha = 0.07$; (\circ) $\alpha = 0.10$; (∇) $\alpha = 0.15$. The solid lines represent fits based on the model of flexible wormlike micelles in dilute solutions; the arrow indicates the crossover concentration into the semidilute regime.

polymers to analyze the concentration dependence of M_{app} at higher solute concentrations. In semidilute polymer solutions, the osmotic compressibility $d\Pi/dc$ and thus the apparent molar mass scales with concentration c according to a power law as^{3,14}

$$M_{\text{app}} \propto \frac{dc}{d\Pi} \propto c^{1/(1-3\nu)} = c^{-1.31} \quad (2)$$

where the exponent ν has a value $\nu = 0.588$ for polymers in good solvents. The same behavior is expected for wormlike micellar solutions in the semidilute regime. This is indeed observed for the systems with solute oil content $\alpha \leq 0.10$ in a concentration range of approximately $0.02\text{--}0.08 \text{ g cm}^{-3}$ as seen in Figure 5. Linear regression of the experimental data in this concentration range yields a best-fit value $\nu = 0.58 \pm 0.01$ for all data sets ($\alpha \leq 0.10$), in excellent agreement with the value predicted for polymers in good solvents. The data for $\alpha = 0.10$ indicate a crossover to a growth law as $M_{\text{app}} \propto c_m^x$ with $x \approx -1.9$ for concentrations above $c_m > 0.08 \text{ g cm}^{-3}$. A similar behavior was observed by Kato et al.¹⁴ in aqueous solutions of C₁₂E₅ and has been attributed to a crossover into the semidilute Θ -region where the osmotic compressibility scales with concentration according to eq 2, but now with the Θ -exponent $\nu = 0.5$, corresponding to $x = -2$. Figure 5 also reveals that at very low solute concentrations ($c_m < 2 \text{ mg cm}^{-3}$) the increase in M_{app} follows a power law as well. In this regime, the structure factor $S(c_m, q = 0)$ is essentially unity and the apparent mass is close to the real micellar mass M_w . For all quasi-binary data sets of low solute oil content and for the binary system C₁₂E₅–water (not shown in the plot) the increase in M_{app} conforms with the mean-field power law $M_w \propto c_m^{0.5}$ in this low concentration regime.

While in the highly diluted and semidilute regime the concentration dependence of M_{app} is well described by the

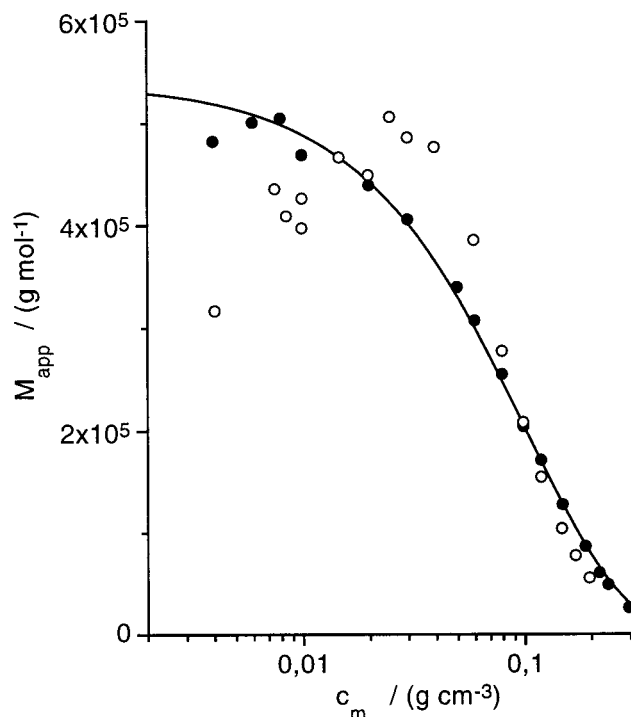


Figure 4. M_{app} vs c_m for $\alpha = 0.25$ (\circ) and $\alpha = 0.35$ (\bullet) at 22 °C. The full line is a fit to the data of $\alpha = 0.35$ for a hard-sphere system.

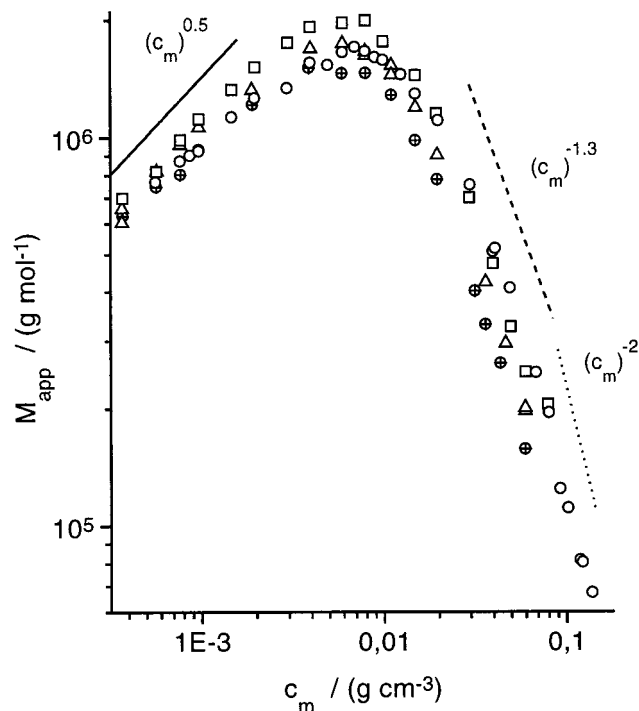


Figure 5. M_{app} vs c_m for $0.02 \leq \alpha \leq 0.10$ at 22 °C in a double-logarithmic plot. The prediction for $M_{\text{app}} \propto c_m^x$ for the semidilute ($x = -1.3$) and the semidilute Θ -region ($x = -2$) are indicated as dashed and dotted lines. The solid line illustrates the mean-field prediction $M_{\text{app}} \propto c_m^{0.5}$ at low c_m . Symbols: (\oplus) $\alpha = 0.02$; (Δ) $\alpha = 0.05$; (\square) $\alpha = 0.07$; (\circ) $\alpha = 0.10$.

predicted power laws, a more sophisticated model has to be applied in the intermediate concentration regime where the power law exponent x changes sign. In this region the structure factor $S(c_m, q = 0)$ of the micellar solution has to be considered when analyzing the concentration dependence of M_{app} . An appropriate expression for eq 1 for solutions of wormlike micelles is obtained by a combination of the structure factor

TABLE 2: Best Fit Values of the Growth Exponent a and the Prefactors B and D of Eqs 4 and 3, Respectively, Using $\nu = 0.588^a$

α	0	0.02	0.05	0.07	0.10	0.15
a	0.53	0.52	0.53	0.56	0.49	(0.53)
$B, 10^7 \text{ g}^{(1-a)} \text{ cm}^{3a} \text{ mol}^{-1}$	3.6	3.8	4.4	5.6	3.0	(1.9)
$D, 10^{-4} \text{ cm}^3 \text{ mol}^{0.764} \text{ g}^{-1.764}$	8.4	5.8	4.9	4.3	4.1	(2.9)
$\Delta T, \text{ K}$	9.8	9.0	6.2	4.7	4.7	5.1

^a The quantity ΔT represents the distance of the experimental temperature ($T = 22^\circ \text{C}$) from the phase separation temperature at the given oil content α (cf. Figure 1).

for flexible polymers in (semi)dilute solutions with a power law for the concentration dependence of the micellar growth.⁹ According to renormalization group theory, $S(c, q = 0)$ for flexible polymers in good solvents depends on a reduced concentration variable X only.²² For polydisperse polymers with an exponential chain length distribution this reduced concentration is given by $X = 2.1cA_2M_w$, where c is again the mass concentration and A_2 is the second osmotic virial coefficient. A_2 depends on the mean-square radius of gyration $\langle R_g^2 \rangle$ and the molar mass M_w ,

$$A_2 \propto \frac{\langle R_g^2 \rangle^{1.5}}{M_w^2}$$

and can be expressed in terms of M_w alone by inserting a scaling relation $R_g \sim M^\nu$ with the good solvent exponent $\nu = 0.588$. The resulting power law

$$A_2 = DM_w^{3\nu-2} \quad (3)$$

allows the calculation of the reduced concentration X , the structure factor $S(c, q = 0)$, and the apparent molar mass M_w for a given concentration c .

This method can be adapted to wormlike micellar systems by introducing the power-law concentration dependence of M_w into eq 1 and 3

$$M_w = Bc_m^a \quad (4)$$

In terms of this application of renormalization group theory to micellar systems, the apparent molar mass is only a function of the experimental solute concentration c_m and three adjustable parameters, viz., the system-specific prefactors B and D of eqs 3 and 4 and the growth exponent a :

$$M_{\text{app}} = F(B, D, a, c_m) \quad (5)$$

It has been demonstrated that the concentration dependence of the apparent molar mass can be represented by eq 5 for such different systems as C_{16}E_6 in D_2O ⁷ or lecithin reverse micelles.⁹ However, in both cases a satisfactory fit was possible only by adopting an exponent a in the power law (eq 4) significantly higher than the expected mean field value $a \approx 0.5$.

We applied this ansatz to analyze the concentration dependence of the apparent molar mass for the solute mixtures with $\alpha \leq 0.10$ in the dilute region. The exponent ν in the scaling relation $R_g \sim M^\nu$ was fixed at $\nu = 0.588$ in accordance with the result from the scaling analysis of M_{app} in the semidilute regime. The results of this analysis are shown by the full curves in Figures 2 and 3, and the resulting parameters B , D , and a are summarized in Table 2. For concentrations up to $c_m \leq 0.02 \text{ g cm}^{-3}$, all data sets can be represented within experimental accuracy by the model of flexible wormlike micelles in dilute solution. For all data sets, we find a growth exponent $a \approx 0.5$,

as predicted by mean-field theory. At concentrations higher than $c_m \approx 0.02 \text{ g cm}^{-3}$, corresponding to a reduced concentration of $X \approx 3$, the model functions deviate from the data. This indicates the crossover from the dilute into the semidilute regime, for which a higher growth exponent ($a \approx 0.6$) is predicted.^{1,2} Note that the scaling analysis presented above indicates the crossover into the semidilute regime at about the same solute concentration (Figure 5). Due to the rather complex interdependence of the parameters in eq 5 a satisfactory description of the experimental data in the entire concentration range is not possible with a single set of parameters.

The prefactor B in eq 4 is a direct measure for the micellar mass M_w . Comparison of the results in Table 2 reveals a strong dependence of the micellar mass on the solute oil content α . Since we lack knowledge of the real length and thickness of the wormlike micelles, we discuss this result only in qualitative terms at this stage. At a given concentration c_m , the mean micellar mass M_w is the product of the mass per unit length M_L and the mean length \bar{L} of the micelles. Both quantities depend on the oil content α of the micelles: M_L will increase with α as the oil molecules are expected to be solubilized in the core of the cylindrical micelles, thus causing an increase of the (cross-sectional) radius of the cylinder. On the other hand, theory predicts an exponential dependence of the mean length \bar{L} of the wormlike micelles on the surfactant film properties and the cylindrical radius of the micelles,²³ viz.,

$$\bar{L} \propto \exp\left(\frac{k'}{4k_B T}\right)$$

where k' is related to the energy difference between hemispherical end caps and the cylindrical body of the micelle and decreases with the product of the cylinder radius and the surfactant film curvature c_0 . With increasing solute oil content α the increase of the cylinder radius will lower k' , thus diminishing the driving force for anisometric growth. This effect will lead to a rapid decrease in the mean micellar length at a given concentration c_m when more oil is incorporated into the wormlike micelles. Together with the increase in M_L with α , this simple view can explain a maximum in M_w at low solute oil content. To distinguish between both effects on M_w with increasing α , the variation of M_L with the solute oil content has been investigated by small angle neutron scattering experiments. Results of this study will be presented elsewhere.²⁴

As seen in Table 2, the prefactor D in eq 3 decreases with increasing oil content of the solute at low α . In terms of the applied model this corresponds to a decrease of A_2 when oil is incorporated into the micelles at the chosen experimental temperature. This decrease of D (i.e., A_2) with increasing α parallels the temperature increment $\Delta T = T_{\text{min}} - T$, where T_{min} represents the minimum of the phase separation curve at the given oil content, and T is the experimental temperature (see Table 2). This is in line with the results of a light scattering study of semidilute aqueous solutions of C_{12}E_5 in D_2O by Kato et al.,¹⁴ where they pointed at the analogy of their system and polymer solutions exhibiting a lower critical solution point. They concluded that in the $\text{C}_{12}\text{E}_5 + \text{D}_2\text{O}$ system a θ -temperature ($A_2 = 0$) exists at ca. $3.5\text{--}0.5 \text{ K}$ below the phase separation curve. Accordingly, the increase of solute oil content will lead to smaller values of A_2 as the Θ -temperature is approached.

To this respect, the analysis of the apparent molar masses using expressions derived for polymers in good solvents with a fixed scaling exponent $\nu = 0.588$ may be questionable. However, as has been established experimentally, the predictions of the renormalization group theory may apply as well to

polymers in marginal solvents or to comparatively stiff polymers up to a reduced concentration $X \approx 3$.¹⁵ Since higher reduced concentrations are not covered in the description of our experimental data within the model, we believe our approach to be valid. As regards the constant value of the scaling exponent ν in $R_g \sim M^\nu$ in our analysis, a decrease of the solvent quality induced by lowering ΔT will cause a shift from the value $\nu = 0.588$ for good solvents toward the value at Θ -conditions ($\nu = 0.5$). On the other hand, with increasing α the oil-swollen wormlike micelles become intrinsically stiffer, which in turn will cause an increase in ν . From the analysis of the scaling behavior in the semidilute regime it is evident that ν is essentially constant, showing that the two parameters influencing ν apparently balance each other. Thus, it appears to be justified to analyze the data with $\nu = 0.588$ independently of α , as in the present work.

The competition of micellar growth and thermodynamic properties which both determine the reduced concentration X in the structure factor $S(q=0)$ leads to the observed variation of the maximum position of $M_{app}(c_m)$ with increasing α . The maximum in M_{app} results from the rapid decrease of the structure factor at higher reduced concentrations $X \propto c_m A_2 M_w$. At $\alpha \leq 0.07$, the molar mass M_w is increasing with α , and one would expect a shift of the maximum of M_{app} to lower solute concentrations since the same reduced concentration X is reached at lower solute concentrations. However, the increase in micellar mass M_w with α is overruled by the decrease in A_2 , and the maximum in M_{app} is shifted to a higher concentration (Figure 2). At $\alpha = 0.10$, the maximum is again shifted to a higher concentration compared to $\alpha = 0.07$ (Figure 3), but this is due to the decrease in micellar mass M_w .

High Solute Oil Content. Figure 3 and 4 show the results for M_{app} vs c_m for the composition scans at higher oil content of the solute ($\alpha \geq 0.07$). In this regime the effect of an increase in α on M_{app} is opposite to that in the low oil content region, indicating a crossover to a different aggregate structure. For $\alpha = 0.15$, we find a semidilute regime at solute concentrations $0.04 \text{ g cm}^{-3} \leq c_m \leq 0.08 \text{ g cm}^{-3}$ and the semidilute Θ -region at $c_m \geq 0.08 \text{ g cm}^{-3}$. This follows from the observation that M_{app} scales with the solute concentration according to $M_{app} \propto c_m^x$ with $x \approx -1.4$ and $x \approx -2$, respectively, in these two regions of c_m . On the other hand, at the lowest experimental concentrations at $\alpha = 0.15$ M_{app} is considerably lower than in the regime of $\alpha \leq 0.10$. No satisfactory fit to the data within the model of wormlike micelles can be achieved over the whole concentration range of the dilute regime $c_m \leq 0.04 \text{ g cm}^{-3}$, and significant deviations occur at higher concentrations but still below the crossover into the semidilute regime (Figure 4). Nevertheless, the increase in M_{app} with c_m follows the mean-field power law at low solute concentrations, and the results of the fitting procedure based on eq 5 are included in Table 2 to point out the decrease in molar mass with increasing oil content of the solute.

At $\alpha = 0.25$, the crossover to comparatively small oil-swollen micelles is reflected by the fact that M_{app} in dilute solutions is now much lower than in the region of wormlike micelles. The increase of M_{app} with c_m at low concentration is only weak and can be interpreted as a moderate growth of small micelles. A quantitative analysis of the concentration dependence of M_{app} is not possible, because we lack a model for the micellar growth and an expression for the structure factor $S(c_m, q=0)$. Finally, at $\alpha = 0.35$ M_{app} exhibits an almost monotonic decrease with increasing c_m . Note that at the lowest concentrations M_{app} is higher than at $\alpha = 0.25$. Neglecting the influence of the structure

factor, this finding is in accordance with the model of weak anisometric micelles, since for spherical oil-swollen micelles the molar mass will increase with the oil-to-surfactant ratio α . The monotonic decrease in M_{app} vs c_m at $\alpha = 0.35$ suggests that a droplet microemulsion is formed. Modeling the oil-swollen micelles as spherical particles of constant size, independent of the solute concentration c_m , we may apply a hard-sphere model with the Carnahan–Starling expression for the structure factor $S_{CS}(\phi_{hs}, q=0)$,²⁵

$$M_{app} = M_w S_{CS}(\phi_{hs}, q=0) = M_w \frac{(1 - \phi_{hs})^4}{1 + 4\phi_{hs} + 4\phi_{hs}^2 - 4\phi_{hs}^3 + \phi_{hs}^4} \quad (6)$$

where ϕ_{hs} represents the volume fraction of the hard-sphere particles. Since it is known that ϕ_{hs} is not always equivalent to the solute volume fraction,¹⁸ we use $\phi_{hs} = \gamma c_m$ to calculate the hard sphere volume fraction from the solute mass concentration and treat the unknown constants γ and M_w as fit parameters. As can be seen from Figure 4, the hard-sphere model provides a satisfactory fit of the data at $\alpha = 0.35$ over almost the whole concentration range; with $M_w = 5.4 \times 10^5 \text{ g/mol}$ and $\gamma = 1.25 \text{ cm}^3/\text{g}$. From these best fit values we derive a hard-sphere radius of $R_{hs} \approx 6.4 \text{ nm}$. This value is consistent with the hydrodynamic radius at zero concentration, $R_h \approx 6.8 \text{ nm}$, from dynamic light scattering experiments. Accordingly, we may conclude that at a mass fraction of $\alpha = 0.35$ in the oil plus surfactant mixture (corresponding to a molar ratio of oil to surfactant of 3:2) the crossover from oil-swollen wormlike micelles to spherical microemulsion droplets has come to completion.

4. Conclusion

We have performed static light scattering experiments on aqueous solutions of C₁₂E₅–decane mixtures in the isotropic micellar L₁ phase. The micellar structure was tuned by varying the mass fraction of decane of the solute, α , at constant temperature (22 °C). At low solute oil content ($\alpha \leq 0.10$), the concentration dependence of M_{app} in the dilute regime is consistent with a model of wormlike micelles that grow according to the mean-field prediction $M_w \propto c_m^a$ with $a \approx 0.5$. At higher solute concentrations the micelles entangle and the osmotic compressibility scales with concentration in analogy to semidilute polymer solutions. The micellar mass M_w exhibits a maximum near $\alpha = 0.07$ and decreases rapidly when the oil content of the micelles is further increased. This experimental result can be understood qualitatively when considering the variation of the mass per unit length M_L and of the mean micellar length \bar{L} with the solute oil content. To disentangle the contribution of M_L and \bar{L} on the micellar mass M_w , the variation of M_L with α has to be determined by small angle neutron scattering, which is the subject of our present work. A crossover from wormlike micelles to less anisometric micelles occurs within a region of 10–25% solute oil content. At $\alpha = 0.25$, the micellar growth with c_m is no longer pronounced, and at 35% solute oil content a droplet microemulsion of constant droplet size is found in which oil-swollen globular micelles interact with each other like hard spheres.

References and Notes

- (1) Cates, M. E.; Candau, S. J. *J. Phys.: Condens. Matter* **1990**, *2*, 6869.
- (2) Wittmer, J. P.; Milchev, A.; Cates, M. E. *Europhys. Lett.* **1998**, *41*, 291.

- (3) Porte, G. In *Micelles, Membranes, Microemulsions, and Monolayers*; Gelbart, W. M., Ben-Shaul, A., Roux, D., Eds.; Partially Ordered Systems; Springer-Verlag: New York, 1994; Chapter 2.
- (4) Kato, T.; Kanada, M.; Seimiya, T. *Langmuir* **1995**, *11*, 1867.
- (5) Buhler, E.; Munch, J. P.; Candau, S. J. *J. Phys. II (Paris)* **1995**, *5*, 765.
- (6) von Berlepsch, H.; Dautzenberg, H.; Rother, G.; Jäger, J. *Langmuir* **1996**, *12*, 3613.
- (7) Schurtenberger, P.; Cavaco, C.; Tiberg, F.; Regev, O. *Langmuir* **1996**, *12*, 2894.
- (8) van der Schoot, P.; McDonald, J. A.; Rennie, A. R. *Langmuir* **1995**, *11*, 4614.
- (9) Schurtenberger, P.; Cavaco, C. *J. Phys. II* **1993**, *3*, 1279.
- (10) Kato, T.; Anzai, S.; Takano, A.; Seimiya, T. *J. Chem. Soc., Faraday Trans. I* **1989**, *85*, 2499.
- (11) Nilsson, P.-G.; Wennerström, H.; Lindman, B. *Chem. Scr.* **1985**, *25*, 67.
- (12) Brown, W.; Pu, Z.; Rymden, R. *J. Phys. Chem.* **1988**, *92*, 6086.
- (13) Glatter, O.; Strey, R.; Schubert, K.-V.; Kaler, E. W. *Ber. Bunsen-Ges. Phys. Chem.* **1996**, *100*, 323.
- (14) Kato, T.; Anzai, S.; Seimiya, T. *J. Phys. Chem.* **1990**, *94*, 7255.
- (15) Burchard, W. *Prog. Colloid Polym. Sci.* **1988**, *78*, 63.
- (16) Schubert, K.-V.; Strey, R.; Kahlweit, M. *J. Colloid Interface Sci.* **1991**, *141*, 21.
- (17) Leaver, M. S.; Olsson, U.; Wennerström, H.; Strey, R.; Würz, U. *J. Chem. Soc., Faraday Trans.* **1995**, *91*, 4269.
- (18) Olsson, U.; Schurtenberger, P. *Langmuir* **1993**, *9*, 3389.
- (19) Gompper, G.; Schick, M. In *Self-Assembling Amphiphilic Systems*; Domb, C., Lebowitz, J. L., Eds.; Phase Transitions and Critical Phenomena, Vol. 16; Academic Press: London, 1994; p 144.
- (20) Strey, R. *Ber. Bunsen-Ges. Phys. Chem.* **1996**, *100*, 182.
- (21) Chu, B. *Laser Light Scattering*, 2nd ed.; Academic Press: San Diego, 1991.
- (22) Ohta, T.; Oono, Y. *Phys. Lett.* **1982**, *89A*, 460.
- (23) Safran, S. A. In *Micelles, Membranes, Microemulsions, and Monolayers*; Gelbart, W. M., Ben-Shaul, A., Roux, D., Eds.; Partially Ordered Systems; Springer-Verlag: New York, 1994; Chapter 9.
- (24) Menge, U.; Lang, P.; Findenegg, G. H. Manuscript in preparation.
- (25) Carnahan, N. F.; Starling, K. E. *J. Chem. Phys.* **1969**, *51*, 635.